Full length article

G protein-coupled estrogen receptor activation by bisphenol-A disrupts the protection from apoptosis conferred by the estrogen receptors ERα and ERβ in pancreatic beta cells

Ignacio Babiloni-Chust [a,b,1], Reinaldo S. dos Santos [a,b,1], Regla M. Medina-Gali [a,b], Atenea A. Perez-Serna [a,b], José-Antonio Encinar [a], Juan Martinez-Pinna [c,a], Jan-Ake Gustafsson [d,e], Laura Marroqui [a,b], Angel Nadal [a,b,*]

[a] Instituto de Investigación, Desarrollo e Innovación en Biotecnología Sanitaria de Elche (IDiBE), Universidad Miguel Hernández de Elche, Elche, Spain
[b] Centro de Investigación Biomédica en Red de Diabetes y Enfermedades Metabólicas Asociadas (CIBERDEM), Spain
[c] Departamento de Fisiología, Genética y Microbiología, Universidad de Alicante, Alicante, Spain
[d] Department of Cell Biology and Biochemistry, Center for Nuclear Receptors and Cell Signaling, University of Houston, Houston, TX, USA
[e] Department of Biosciences and Nutrition, Karolinska Institutet, Huddinge, Sweden

ARTICLE INFO

ABSTRACT

17β-estradiol protects pancreatic β-cells from apoptosis via the estrogen receptors ERα, ERβ and GPER. Conversely, the endocrine disruptor bisphenol-A (BPA), which exerts multiple effects in this cell type via the same estrogen receptors, increased basal apoptosis. The molecular-initiated events that trigger these opposite actions have yet to be identified. We demonstrated that combined genetic downregulation and pharmacological blockade of each estrogen receptor increased apoptosis to a different extent. The increase in apoptosis induced by BPA was diminished by the pharmacological blockade or the genetic silencing of GPER, and it was partially reproduced by the GPER agonist G1. BPA and G1-induced apoptosis were abolished upon pharmacological inhibition, silencing of ERα and ERβ, or in dispersed islet cells from ERβ knockout (BERKO) mice. However, the ERα and ERβ agonists PPT and DPN, respectively, had no effect on beta cell viability. To exert their biological actions, ERα and ERβ form homodimers and heterodimers. Molecular dynamics simulations together with proximity ligand assays and coimmunoprecipitation experiments indicated that the interaction of BPA with ERα and ERβ as well as GPER activation by G1 decreased ERαβ heterodimers. We propose that ERαβ heterodimers play an antiapoptotic role in beta cells and that BPA- and G1-induced decreases in ERαβ heterodimers lead to beta cell apoptosis. Unveiling how different estrogenic chemicals affect the crosstalk among estrogen receptors should help to identify diabetogenic endocrine disruptors.

1. Introduction

Loss of functional beta cell mass is a critical component contributing to the hyperglycemia observed in individuals with type 1 or type 2 diabetes. The interaction between the individual genetic background and environmental factors determines the progression of beta cell dysfunction and death (Eizirik et al., 2020).

Sex differences exist in the prevalence of diabetes. Premenopausal women have a lower incidence of diabetes than men (Gannon et al., 2018; Kautzky-Willer et al., 2016). These sex differences can be partially attributed to the action of 17β-estradiol (E2) through three estrogen receptors (ERs), i.e., estrogen receptors α (ERα) and β (ERβ) (Heldring et al., 2007) and the G protein-coupled estrogen receptor (GPER/GPR30) (Revankar et al., 2005; Thomas et al., 2005). After ligand

binding, ERα and ERβ can either form homo and heterodimers and act as transcription factors or tether other DNA-bound transcription factors (Heldring et al., 2007). In addition to their nuclear-initiated actions, ERα and ERβ can trigger extranuclear-initiated effects after dimerization and activate a variety of signaling pathways (Levin and Hammes, 2016).

All three ERs protect beta cells from different apoptotic insults (Balhuizen et al., 2010; le May et al., 2006; Liu et al., 2009), yet the role of E2 can be disrupted by environmental chemicals that compete for the same receptors and modify the physiological pathways activated by the natural hormone (Gore et al., 2015). Bisphenol-A (BPA), which is used as a model of endocrine disrupting chemicals that alter insulin secretion and insulin sensitivity in mice (Alonso-Magdalena et al., 2010, 2006), has been implicated in the etiology of diabetes (Alonso-Magdalena et al., 2011; Sargis and Simmons, 2019). At concentrations similar to those found in human blood (Vandenberg et al., 2010), BPA increases pancreatic insulin content via ERα (Alonso-Magdalena et al., 2008) and regulates ion channel expression and function as well as augments insulin release in an ERβ-mediated manner (Marroqui et al., 2021; Martinez-Pinna et al., 2019; Soriano et al., 2012). In INS-1 cells and mouse dispersed islet cells, BPA induces mitochondrial dysfunction, ROS production and NF-κB activation, which culminates in beta cell apoptosis (Carchia et al., 2015; Lin et al., 2013).

Because E2 and BPA have opposite actions on beta cell survival, we decided to investigate the molecular initiating event (MIE) (Allen et al., 2014) underlying the pro-apoptotic effect of BPA. Using several beta cell models, including the EndoC-βH1 cell line, which is a model of human beta cells recommended for screening studies (Tsonkova et al., 2018), we show that ERα, ERβ and GPER mediate beta cell survival. Our findings suggest that ERαβ heterodimerization is key to this antiapoptotic role and that G1, a GPER agonist, and BPA induce apoptosis via a mechanism involving the reduction in ERαβ heterodimers downstream of GPER.

2. Materials and methods

2.1. Chemical substances and animals

Bisphenol-A was purchased from MP Biomedicals (Cat no. 155118; Santa Ana, CA, USA). 17β-Estradiol (E2, Cat no. E8875) was obtained from Sigma–Aldrich (Saint Louis, MO, USA). Propylpyrazoletriol (PPT, Cat no. 1426), diarylpropionitrile (DPN, Cat no. 1494), G1 (Cat no. 3577), ICI 182,780 (Cat no. 1047), PHTPP (Cat no. 2662) and methyl-piperidinopyrazole (MPP, Cat no. 1991) were obtained from Tocris Cookson (Bristol, UK).

Mice with knockout of the *Erβ* gene (also known as *Esr2*) (BERKO mice), supplied by Jan-Åke Gustafsson's laboratory, were generated as previously described (Krege et al., 1998). Wild-type littermates and BERKO mice were obtained from the same supplier and colony and kept under standard housing conditions (12 h light/dark cycle, food *ad libitum*). Experimental procedures were performed according to the Spanish Royal Decree 1201/2005 and the European Community Council directive 2010/63/EU. The ethical committee of Miguel Hernandez University reviewed and approved the methods used herein (approval IDs: UMH-IB-AN-01–14 and UMH-IB-AN-02-14).

2.2. Culture of cell lines and dispersed islet cells

Rat insulin-producing INS-1E cells (RRID: CVCL_0351, kindly provided by Dr. C. Wollheim, Department of Cell Physiology and Metabolism, University of Geneva, Geneva, Switzerland) were cultured as previously described (Santin et al., 2016). Human insulin-producing EndoC-βH1 cells (RRID: CVCL_L909, Univercell-Biosolutions, France) were cultured in Matrigel/fibronectin-coated plates as previously described (Ravassard et al., 2011). INS-1E and EndoC-βH1 cells have been shown to be free of mycoplasma infection. Pancreatic islets were isolated using collagenase (Sigma, St Louis, MO, USA) as previously described (Alonso-Magdalena et al., 2008). Islets were dispersed into single cells and cultured in polylysine-coated plates as previously described (Martinez-Pinna et al., 2019). Cell lines and dispersed cells were kept at 37 °C in a humidified atmosphere of 95% O_2 and 5% CO_2.

2.3. RNA interference

The optimal siRNA concentration (30 nM) and conditions for small interfering RNA (siRNA) transfection using Lipofectamine RNAiMAX lipid reagent (Invitrogen, Carlsbad, CA, USA) were previously established (Santin et al., 2016). Allstars Negative Control siRNA (Qiagen, Venlo, the Netherlands) was used as a negative control (siCTRL). siRNA targeting *Erα* (also known as *Esr1*; si*ERα*), *Erβ* (si*ERβ*) or *Gper1* (si*GPER1*) (Qiagen, Venlo, the Netherlands) were used herein (Supplementary Table 2). Of note, GPER silencing in INS-1E cells as well as ERα and ERβ silencing in EndoC-βH1 cells were performed in a two-step transfection protocol (Marroqui et al., 2015). Briefly, cells were exposed to 30 nmol/l siCTRL or si*GPER1*/si*Gper1* for 16 h, washed and allowed to recover in culture for 24 h. Next, cells were exposed again to the same siRNAs for 16 h, allowed to recover in culture for 48 h, and then used for the subsequent experiments. Transfection with siRNAs was performed in BSA- and antibiotic-free medium.

2.4. Cell viability assessment by DNA-binding dyes

The percentage of apoptosis was determined after staining with the DNA-binding dyes Hoechst 33,342 and propidium iodide as previously described (Santin et al., 2016). To avoid bias, cell viability was assessed by two different observers, one of whom was unaware of the sample identity. The agreement of results between both observations was higher than 90%.

2.5. Flow cytometric analysis

Apoptotic cells were analyzed by flow cytometry using the FITC Annexin V Apoptosis Detection Kit with propidium iodide (BioLegend, San Diego, CA, USA) following the manufacturer's instructions. Briefly, INS-1E cells were detached and dissociated using Accutase (Thermo Fisher Scientific). The cell suspension was washed twice with PBS (200 *g* for 7 min) and subjected to Annexin V-fluorescein isothiocyanate (FITC)/PI staining according to the manufacturer's instructions (FITC Annexin V Apoptosis Detection Kit with PI; BioLegend, San Diego, CA, USA). Cells stained with Annexin V (both Annexin V$^+$- and Annexin V$^+$/PI$^+$-cells) were detected using a FACSCanto II (BD Biosciences, Madrid, Spain) flow cytometer.

2.6. Caspase 3/7 activity

Caspase 3/7 activity was determined using the Caspase-Glo® 3/7 assay (Promega, Madison, WI, USA) following the manufacturer's instructions. Briefly, following treatment, cells were incubated with Caspase-Glo® 3/7 reagent at room temperature before luminescence was recorded with a POLASTAR plate reader (BMG Labtech, Germany).

2.7. MTT assay

Cell viability was measured by the colorimetric assay showing reduction of MTT (3-(4,5-dimethylthiazol-2-yl)-2,5-diphenyltetrazolium bromide) (Sigma–Aldrich) as previously described (Denizot and Lang, 1986; Mosmann, 1983). Briefly, MTT prepared in RPMI 1640 without phenol red was added (final concentration: 0.5 mg/ml) and incubated at 37 °C for 3 h. Upon incubation, the supernatant was aspirated, and 100 ml of DMSO was added to dissolve formazan crystals. The absorbance was measured at 595 nm using an iMark™ Microplate absorbance reader (Bio–Rad, Hercules, CA), and the percentage of cell viability was calculated.

2.8. Real-time PCR

Quantitative RT–PCR was performed in a CFX96 Real-Time System (Bio–Rad Laboratories, Hercules, CA, USA). RNA was extracted with the RNeasy Micro kit (Qiagen), and cDNA was prepared with the High-Capacity cDNA Reverse Transcription kit (Applied Biosystems, Foster City, CA, USA). Amplification reactions were performed as previously described (Villar-Pazos et al., 2017). Values were analyzed with CFX Manager Version 1.6 (Bio–Rad) and expressed as the relative expression with respect to control values ($2^{-\Delta\Delta Ct}$) (Schmittgen and Livak, 2008). *Gapdh* and β-actin were used as housekeeping genes for rat and human samples, respectively. The primers used herein are listed in Supplementary Table 2.

2.9. DCF assay

Oxidative stress was measured using the fluorescent probe 2′,7′-dichlorofluorescein diacetate (DCF; Sigma–Aldrich) as previously described (Cunha et al., 2016). Briefly, cells seeded in 96-well black plates were loaded with 10 µM DCF for 30 min at 37 °C and washed with PBS. DCF fluorescence was quantified in a POLASTAR plate reader (BMG Labtech, Germany). Data are expressed as DCF fluorescence corrected by total protein.

2.10. Western blotting

Cells were washed with cold PBS and lysed in Laemmli buffer. Immunoblot analysis was performed by overnight incubation with antibodies against ERα, ERβ, GPER, β-actin, GAPDH and α-tubulin. Afterward, the membranes were incubated for 1 h at room temperature with peroxidase-conjugated antibodies (1:5000) as secondary antibodies. SuperSignal West Femto chemiluminescent substrate (Thermo Scientific, Rockford, IL, USA) and ChemiDoc XRS+ (Bio–Rad Laboratories) were used to detect immunoreactive bands. Densitometry analysis was performed with Image Lab software (version 4.1, Bio–Rad Laboratories). The antibodies used herein are listed in Supplementary Table 3.

2.11. In situ proximity ligation assay (PLA)

In situ PLA was performed using a Duolink® In Situ Red Starter Kit (Sigma–Aldrich) following the manufacturer's instructions with slight modifications (INCLUDE Iwabuchi E, Miki Y, Ono K, et al., J Steroid Biochem Mol Biol 165:159–169, 2017)(Iwabuchi et al., 2017). Briefly, cells grown on coverslips were washed with PBS and fixed with 4% paraformaldehyde (VWR Chemicals, Spain). Then, the cells were washed with PBS and permeabilized with 0.1% Triton-X-100. Subsequently, the cells were incubated for 30 min at 37 °C with a blocking solution and incubated overnight at 4 °C with the corresponding primary antibodies (Supplementary Table 3). PLA probe solution was added and incubated for 1 h at 37 °C. Ligation-Ligase solution was added, and coverslips were incubated for 30 min at 37 °C. Subsequently, amplification-polymerase solution was added and incubated for 100 min at 37 °C. Of note, all incubations at 37 °C were performed using a pre-heated humidity chamber. Finally, coverslips were washed with a specific buffer and mounted with a minimal volume of Duolink in situ mounting medium with DAPI®. ER dimers were observed using a Zeiss Confocal LSM900 microscope equipped with a camera (Zeiss-Vision, Munich, Germany), and images were acquired at x63 magnification and analyzed using ZEN software (version 3.2; Zeiss-Vision, Munich, Germany).

2.12. Coimmunoprecipitation

INS-1E cells were washed with cold PBS, lysed in cold immunoprecipitation buffer (50 mmol/l Tris, pH 7.5, 4 mmol/l NaCl, 2 mmol/l MgCl$_2$, 10 mmol/l NaF, 1 mmol/l PMSF, 1% Triton X-100 and Complete Protease inhibitor mixture, Roche Diagnostics) for 30 min on ice and centrifuged at 20,000 × g for 10 min at 4 °C. Cell lysates were precleared for 1 h at 4 °C with Dynabeads Protein G (Thermo Fischer Scientific; Cat no. 10003D). The same amounts of protein were incubated overnight at 4 °C, either with an anti-ERβ antibody or nonspecific rabbit IgG (Santa Cruz Biotechnology) used as a negative control. Upon overnight incubation, immunoprecipitates were incubated for 1 h at 4 °C with Dynabeads Protein G, washed six times with cold immunoprecipitation buffer and resuspended in 5x Laemmli buffer. Immunoprecipitates and total protein (input) were subjected to SDS–PAGE and immunoblotted with mouse anti-ERα antibody. The antibodies used herein are listed in Supplementary Table 3.

2.13. Molecular docking and dynamics simulations

More than 300 human ERα-ligand-binding domain (LBD) (UniProt code: P03372) and 32 human ERβ-LBD (UniProt code: Q92731) structures were resolved from cryptographic data. Because these structures contained unresolved residues in mobile regions of the protein that diffracted poorly, the lost amino acids were reconstructed after generation of a homology model at the Swiss-Model server (Biasini et al., 2014; Marroqui et al., 2021). After unresolved gap elimination, models for the hERα-LBD monomer (Protein Data Bank entry 5DXE as template) and the hERβ-LBD monomer (Protein Data Bank entry 3OLS as template) were generated. From these monomeric structures, homo and heterodimers were reconstructed using the GRAMM-X server (Tovchigrechko and Vakser, 2006). E2 and BPA molecular docking simulations within the cavity of each LBD were performed using YASARA structure software (version 20.12.24) (Marroqui et al., 2021). Molecular dynamics simulations of the structures with the best docking calculations were performed with YASARA structure software (version 20.10.24) (Marroqui et al., 2021). The intermolecular protein interaction energy for homo and heterodimer subunits was calculated using Folds 5.0 software (Delgado et al., 2019).

2.14. Statistical analysis

Experimenters were not blinded to group assignment and outcome assessment. GraphPad Prism 7.0 software (GraphPad Software, La Jolla, CA, USA; https://www.graphpad.com) was used for all statistical analyses. Data are expressed as the mean ± SEM. To assess differences between groups, we used two-tailed Student's *t* test or ANOVA when appropriate. For nonparametric data, we used Mann–Whitney and Kruskal–Wallis ANOVA tests (followed by Dunn's test), depending on the experimental groups involved in the comparison. A *p* value ≤ 0.05 was considered to be statistically significant.

3. Results

In INS-1E (Fig. 1a) and EndoC-βH1 cells (Fig. 1b), E2 (10 pM/l to 1 µM) either had no effect or decreased apoptosis. Conversely, BPA increased apoptosis in both cell lines in a dose-dependent manner (Fig. 1c, d). Similar results were observed in dispersed islet cells from female mice (Fig. 1e). These results were confirmed by three other approaches, i.e., flow cytometry analysis (Fig. 1f), caspase 3/7 activity (Fig. 1g) and MTT assay (Supplementary Fig. 1). When E2 and BPA were added together, 1 nM E2 prevented BPA-induced apoptosis (Fig. 1h), suggesting that E2 and BPA initiate common pathways.

Previous work demonstrated that BPA induced oxidative stress in beta cells (Carchia et al., 2015; Lin et al., 2013). Similarly, we observed that BPA upregulated genes encoding the antioxidant enzymes superoxide dismutase (*Sod2*), glutathione peroxidase 4 (*Gpx4*) and catalase (*Cat*) (Supplementary Fig. 2a-c) and increased reactive oxygen species (ROS) generation (Supplementary Fig. 2d, e). The antioxidant N-acetylcysteine abolished BPA-induced ROS production in INS-1E (Supplementary Fig. 2d) and EndoC-βH1 cells (Supplementary Fig. 2e). Of note,
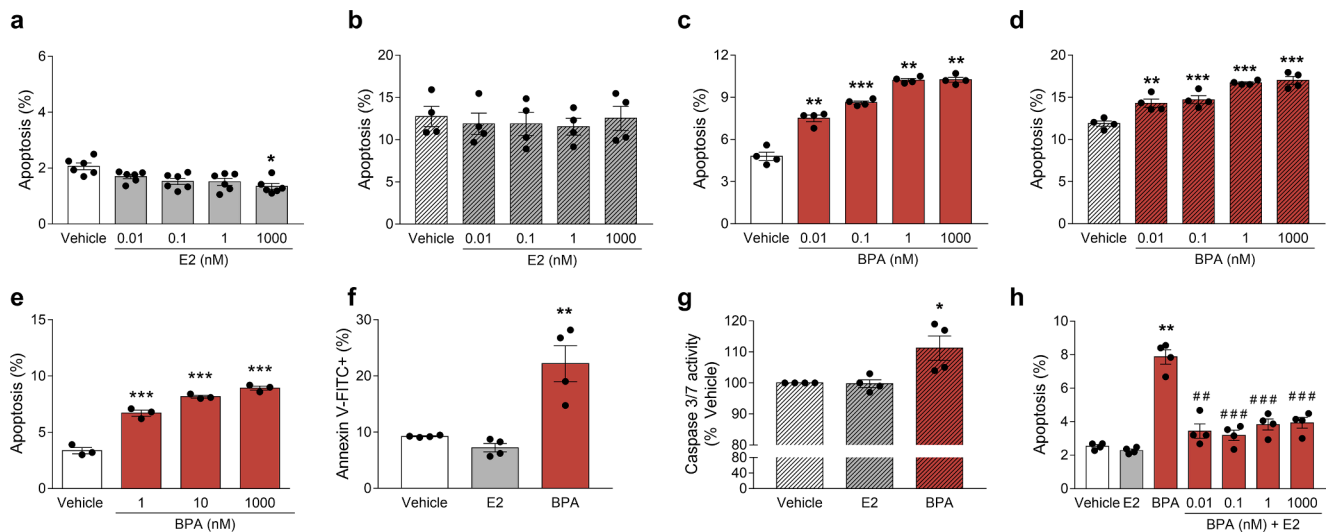
Fig. 1. E2 and BPA have different effects on beta cell viability. INS-1E (**a,c**) and EndoC-βH1 cells (**b,d**) were treated with vehicle (white bars), E2 (grey bars) or BPA (red bars) for 24 h. (**e**) Dispersed islet cells from female mice were treated with vehicle (white bars) or BPA (red bars) for 48 h. Apoptosis was evaluated using Hoechst 33,342 and propidium iodide staining. (**f**) INS-1E cells were treated with vehicle (white bar), E2 1 nM(grey bar) or BPA 1 nM (red bar) for 48 h. Annexin V-FITC-positive cells were analyzed by flow cytometry. (**g**) EndoC-βH1 cells were treated with vehicle (white bar), E2 1 nM (grey bar) or BPA 1 nM (red bar) for 48 h. Caspase 3/7 activity was measured by a luminescent assay. Results are expressed as % vehicle-treated cells. (**h**) INS-1E were treated with vehicle (white bar), E2 1 nM (grey bar), BPA 1 nM (red bar) or a combination of both (red bars + E2) for 24 h. Apoptosis was evaluated using Hoechst 33,342 and propidium iodide staining. Data are shown as means ± SEM of 3–6 independent experiments. (**a-i**) $*p \leq 0.05$, $**p \leq 0.01$ and $***p \leq 0.001$ vs Vehicle, by one-way ANOVA. (**h**) $**p \leq 0.01$ vs Vehicle; $^{\#\#}p \leq 0.01$ and $^{\#\#\#}p \leq 0.001$ vs BPA 1 nM. One-way ANOVA.

N-acetylcysteine prevented BPA-induced apoptosis in both cell lines (Supplementary Fig. 2f, g), reinforcing that oxidative stress is involved in BPA-induced apoptosis. Of note, E2 did not change the ROS levels (data not shown). These results indicate that ROS production is a key event involved in BPA-induced beta cell apoptosis.

Because previous results indicate that BPA acts via ERs in beta cells (Alonso-Magdalena et al., 2008; Martinez-Pinna et al., 2019; Soriano et al., 2012), we evaluated the expression of ERα, ERβ and GPER in INS-1E and EndoC-βH1 cells by quantitative RT–PCR and western blot. Considering ERα expression as 1, mRNA analyses showed that the ratio GPER:ERα:ERβ was 100:1:0.3 for INS-1E cells (Supplementary Fig. 3a) and 675:1:3.3 for EndoC-βH1 cells (Supplementary Fig. 3b). This expression pattern was confirmed at the protein level, where GPER was the most highly expressed of the three receptors (Supplementary Fig. 3c).

3.1. GPER mediates BPA-induced apoptosis

We first assessed whether GPER participated in BPA-induced apoptosis. The GPER antagonist G15 reduced BPA-triggered apoptosis in INS-1E and EndoC-βH1 cells (Fig. 2a, b). Doses as low as 100 pM of the GPER agonist G1 induced apoptosis in INS-1E cells (Supplementary Fig. 4a). In comparison with 1 nM BPA, 100 nM G1 presented a significantly smaller effect on apoptosis in both cell lines (Fig. 2c, d). To further study the role of GPER in beta cell survival, we used siRNAs to inhibit GPER expression in INS-1E and EndoC-βH1 cells (Fig. 2e-j, Supplementary Fig. 4b, c). GPER silencing promoted apoptosis under basal conditions in INS-1E cells but not in EndoC-βH1 cells (Fig. 2f, i). Moreover, GPER-inhibited cells were less susceptible to BPA-induced apoptosis than control cells (Fig. 2f, g, i, j). Similar data were obtained with a second, independent siRNA (data not shown). These results indicate that GPER activation is part of the mechanism whereby BPA elicits apoptosis.

3.2. ERα and ERβ are involved in BPA-induced apoptosis

We then investigated whether ERα and ERβ were also implicated in BPA-induced apoptosis. In both cell lines, the pure antiestrogen ICI

182,780 abolished the BPA effect on apoptosis (Fig. 3a, b). Treatment with the ERα antagonist methylpiperidinopyrazole (MPP) induced apoptosis under basal conditions, while propylpyrazoletriol (PPT), an ERα agonist, did not change viability (Fig. 3c, Supplementary Fig. 5a, b). In INS-1E cells, MPP abolished BPA-induced apoptosis (Fig. 3c). To further characterize ERα participation in cell survival and BPA-induced apoptosis, we silenced ERα expression in INS-1E and EndoC-βH1 cells using specific siRNAs (Fig. 3d, g, Supplementary Fig. 5c-e). ERα knockdown augmented apoptosis under basal conditions and prevented BPA-induced apoptosis in both cell lines (Fig. 3e, f, h, i). We confirmed these data with a second, independent siRNA (data not shown).

Regarding ERβ, while its antagonist 4-(2-phenyl-5,7-bis(tri-fluoromethyl)pyrazolo[1,5-a]pyrimidin-3-yl)phenol (PHTPP) also induced apoptosis under basal conditions, the ERβ agonist diary-lpropionitrile (DPN) had no effect on beta cell viability (Fig. 4a, Supplementary Fig. 6a, b). ERβ inhibition by siRNAs (Fig. 4c, f, Supplementary Fig. 6c-h) induced a substantial increase in apoptosis, mainly in INS-1E cells; importantly, BPA-elicited apoptosis was partially lost following ERβ silencing (Fig. 4d, e, g, h). Comparable results were observed with a second, independent siRNA (data not shown). Finally, the effects of BPA on viability were abrogated in dispersed islet cells from BERKO mice (Fig. 4b).

3.3. Crosstalk among ERα, ERβ and GPER mediates beta cell survival

Because our data indicate that GPER signaling triggers beta cell apoptosis via downstream activation of ERα and ERβ, we sought to examine this hypothesis. First, we observed that G1-induced apoptosis was abolished by the antiestrogen ICI 182,780 (Fig. 5a, b). Because G1 may also bind to and activate a 36-kDa variant of ERα, ERα36 (Kang et al., 2010), we silenced GPER (Fig. 5c, Supplementary Fig. 7a) to test whether G1 affected apoptosis via GPER. Of note, G1 did not affect apoptosis in GPER-silenced cells (Fig. 5d, Supplementary Fig. 7b), indicating that, in our cell system, G1 acts preferentially through GPER. Moreover, MPP (ERα antagonist) and PHTPP (ERβ antagonist) prevented G1-induced apoptosis (Fig. 5e-h). Then, we tested the G1 effects on apoptosis upon silencing ERα or ERβ separately (si*Erα* and si*Erβ*) or
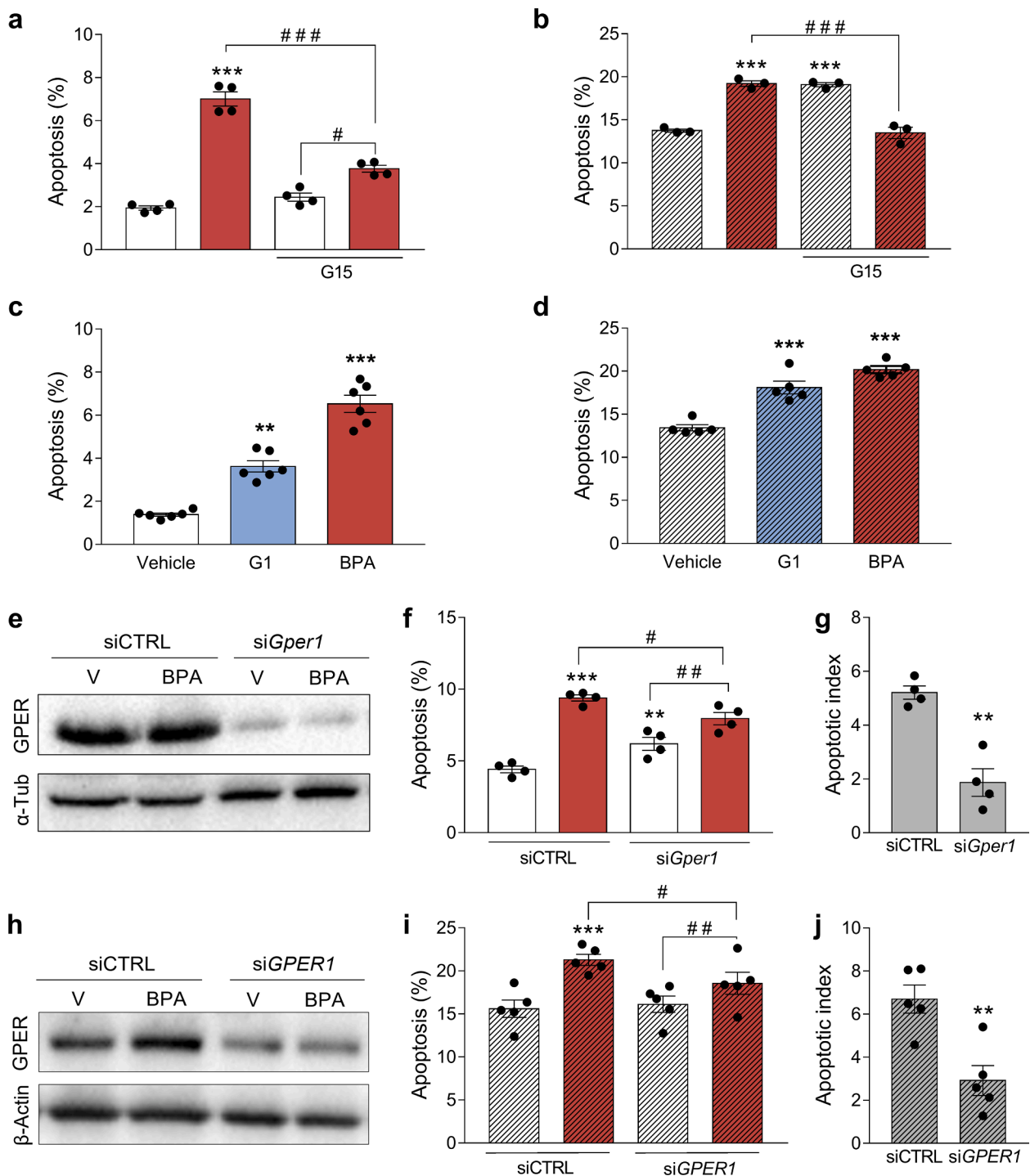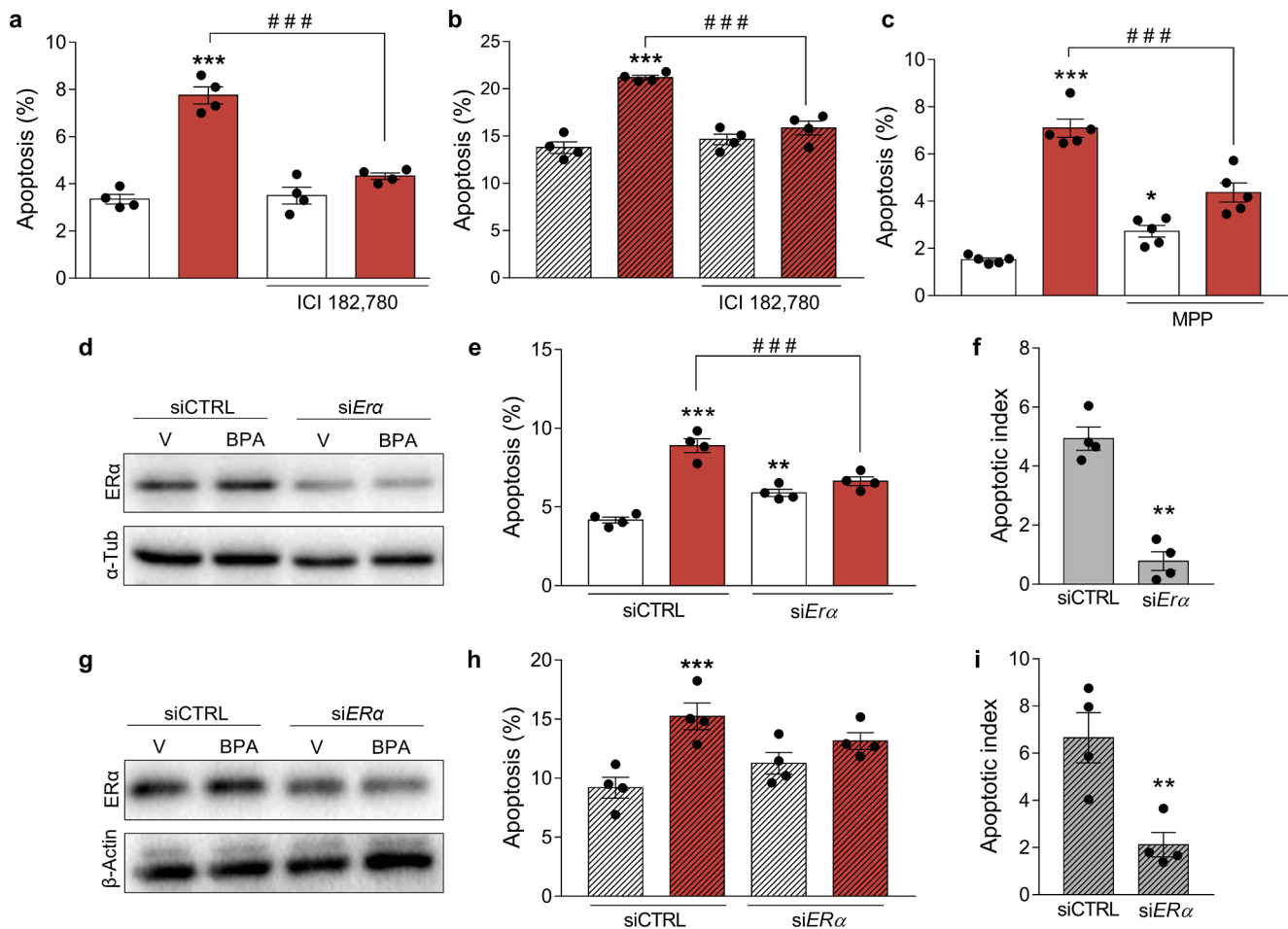
Fig. 2. BPA-induced apoptosis requires GPER. (a,b) INS-1E (**a**) and EndoC-βH1 cells (**b**) were pre-treated with vehicle or GPER antagonist G15 10 nM for 3 h. Afterwards, cells were treated with vehicle (white bars) or BPA 1 nM (red bars) in the absence or presence of G15 10 nM for 24 h. (**c,d**) INS-1E (**c**) and EndoC-βH1 cells (**d**) were treated with vehicle (white bars), G1 100 nM (blue bars) or BPA 1 nM (red bars) for 24 h. Apoptosis was evaluated using Hoechst 33,342 and propidium iodide staining. (**e-j**) INS-1E (**e-g**) and EndoC-βH1 cells (**h-j**) were transfected with siCTRL or with a siRNA targeting GPER (si*Gper1* or si*GPER1*). Cells were treated with vehicle (white bars) or BPA 1 nM (red bars) for 24 h. (**e,h**) Protein expression was measured by western blot. Representative images of four (**e**) or five (**h**) independent experiments are shown. (**f,i**) Apoptosis was evaluated using Hoechst 33,342 and propidium iodide staining. (**g,j**) BPA-induced apoptosis data from Fig. 5f (**g**) and Fig. 5i (**j**) are presented as apoptotic index. Data are shown as means ± SEM of 4–6 independent experiments. (**a,b**) **$p \leq 0.01$ and ***$p \leq 0.001$ vs untreated vehicle; $^{\#\#}p \leq 0.01$, $^{\#\#\#}p \leq 0.001$ as indicated by bars. Two-way ANOVA. (**c,d**) **$p \leq 0.01$ and ***$p \leq 0.001$ vs vehicle, by one-way ANOVA. (**f,i**) **$p \leq 0.01$ and ***$p \leq 0.001$ vs siCTRL vehicle; $^{\#}p \leq 0.05$ and $^{\#\#}p \leq 0.01$ as indicated by bars. Two-way ANOVA. (**g,j**) **$p \leq 0.01$ vs siCTRL, by two-tailed Student's *t* test.

simultaneously (si*Erα/Erβ*) (Fig. 5i, Supplementary Fig. 7c-e). As previously described above, ERα or ERβ knockdown induced beta cell death, and silencing of both receptors simultaneously induced apoptosis to the same extent observed in ERβ-inhibited cells (Fig. 5i,

Supplementary Fig. 7f). The G1 effect on apoptosis was lost in ERα-, ERβ- or ERα/ERβ-deficient cells (Fig. 5i, Supplementary Fig. 7f). In addition, G1 induced apoptosis in dispersed islet cells from WT mice, but its effect on apoptosis was completely blunted in dispersed cells from BERKO

Fig. 3. ERα mediates BPA-induced apoptosis. (**a,b**) INS-1E (**a**) and EndoC-βH1 cells (**b**) were pre-treated with vehicle or antiestrogen ICI 182,780 1 μM for 3 h. Afterwards, cells were treated with vehicle (white bars) or BPA 1 nM (red bars) in the absence or presence of ICI 182,780 1 μM for 24 h. (**c**) INS-1E cells were pre-treated with vehicle or ERα antagonist MPP 100 nM for 3 h. Afterwards, cells were treated with vehicle (white bars) or BPA 1 nM (red bars) in the absence or presence of MPP 100 nM for 24 h. Apoptosis was evaluated using Hoechst 33,342 and propidium iodide staining. (**d-i**) INS-1E (**d-f**) and EndoC-βH1 cells (**g-i**) were transfected with siCTRL or with a siRNA targeting ERα (si*Erα* or si*ERα*). Cells were treated with vehicle (white bars) or BPA 1 nM (red bars) for 24 h. (**d,g**) Protein expression was measured by western blot. Representative images of four independent experiments are shown. (**e,h**) Apoptosis was evaluated using Hoechst 33,342 and propidium iodide staining. (**g,j**) BPA-induced apoptosis data from Fig. 5e (**f**) and Fig. 5h (**i**) are presented as apoptotic index. Data are shown as means ± SEM of 4–5 independent experiments. (**a-c**) *$p \leq 0.05$ and ***$p \leq 0.001$ vs untreated vehicle; ###$p \leq 0.001$ as indicated by bars. Two-way ANOVA. (**e,h**) **$p \leq 0.01$ and ***$p \leq 0.001$ vs siCTRL vehicle; ###$p \leq 0.001$ as indicated by bars. Two-way ANOVA. (**f,i**) **$p \leq 0.01$ vs siCTRL, by two-tailed Student's *t* test.

mice (Fig. 5j). These results indicate that ERβ seems to be more important than ERα for beta cell survival and that ERα and ERβ are required for GPER effects on viability.

3.4. ER heterodimerization

After ligand binding, ERα and ERβ form homodimers and heterodimers to exert their biological actions (Levin and Hammes, 2016; Razandi et al., 2004). Because our data suggest that part of the BPA effect on apoptosis is directly mediated by ERα and ERβ, we sought to study whether the binding of E2 or BPA would stabilize ER homo and/or heterodimers. We performed docking and molecular dynamics simulations using human structural models of ERα and ERβ. Our models were obtained from resolved dimeric structures of the ER LBD where the protein is cocrystallized with ligands E2 and BPA bound to the LBD cavity that is closed by the transactivation helix H12 (Fig. 6a-c). Fig. 6 depicts models of the ERα-ERα homodimer (ERαα; Fig. 6a), ERβ-ERβ homodimer (ERββ; Fig. 6b) and ERα-ERβ heterodimer (ERαβ; Fig. 6c).

Molecular docking simulations resulted in lower Gibbs free energy changes for E2 (-11.05 and −10.86 kcal/mol for hERα-LBD and hERβ-LBD, respectively) compared with BPA (-8.15 and −8.37 kcal/mol for

hERα-LBD and hERβ-LBD, respectively). These values are similar to those observed for rat ERs (Marroqui et al., 2021) and agree with the higher affinity of both receptors for E2 (compared with BPA) (Kuiper et al., 1997). We used these protein–ligand complexes as the starting point to initiate molecular dynamics simulations of the ligands within the cavity for 200 ns. Then, we analyzed the monomer–monomer interaction energy (Fig. 6d-f), the trajectory of the ligands within the LBD pocket (Supplementary Fig. 8) and the solvation binding energy of E2 and BPA bound to the LBD cavity (Fig. 6g-i).

When we examined the monomer–monomer interaction energy with E2 or BPA bound to both cavities of the LBD, we found that for ERαα homodimers, the frequency distribution of the intermolecular interaction energy between monomers was lower for E2 than for BPA (Fig. 6d). This indicates that E2 stabilizes the ERαα homodimer more than BPA. For ERββ homodimers, E2 and BPA presented a similar interaction energy, suggesting comparable ERββ stabilization with both ligands (Fig. 6e). When the interaction energy for ERαβ heterodimers was analyzed, E2 presented a much lower interaction energy than BPA, indicating that BPA does not stabilize heterodimers (Fig. 6f). The trajectory of E2 and BPA within the cavity behaves differently; E2 showed minimal deviations during the 200 ns simulation time for both
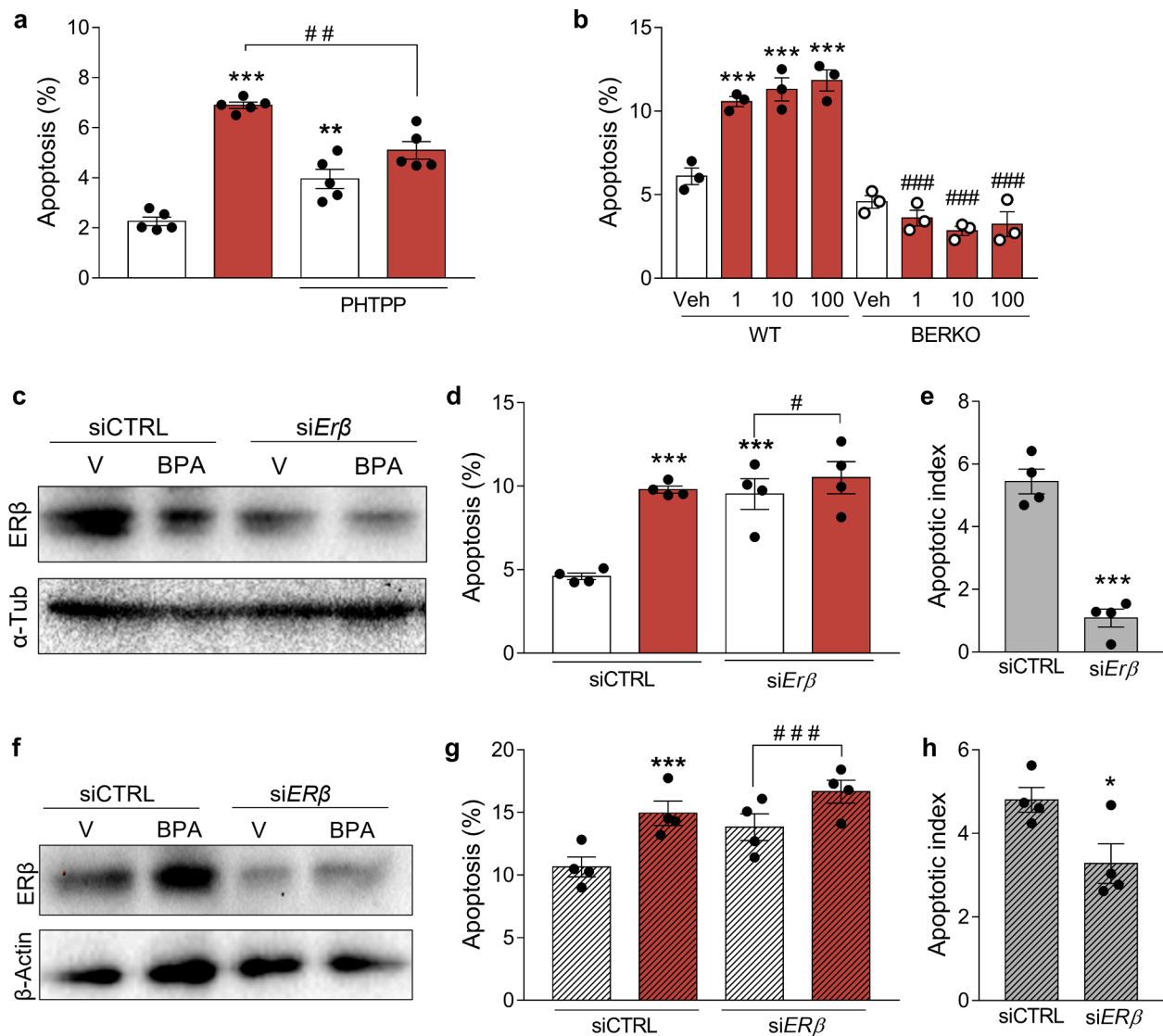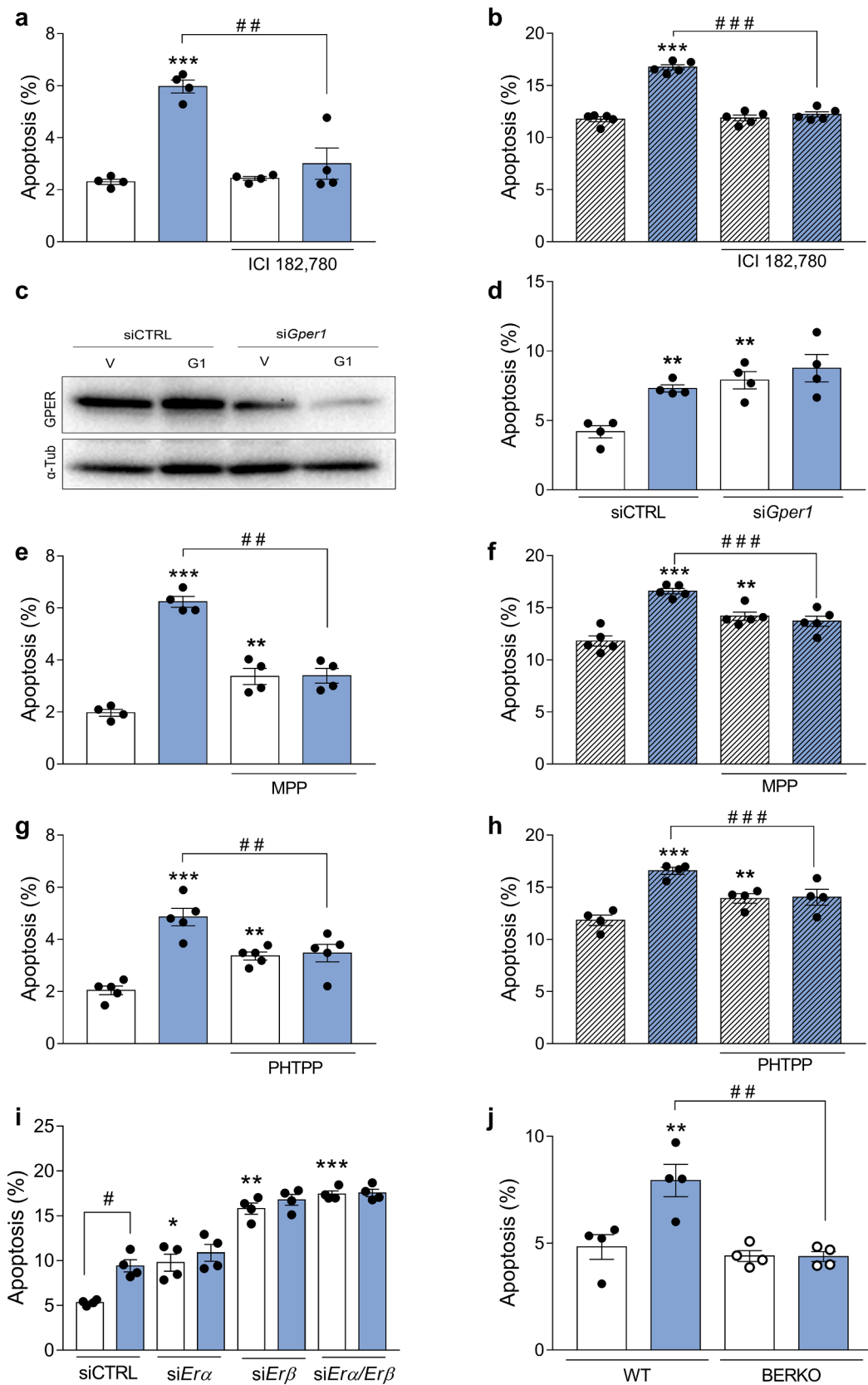
Fig. 4. ERβ mediates BPA-induced apoptosis. (**a**) INS-1E cells were pre-treated with vehicle or ERβ antagonist PHTPP 1 μM for 3 h. Afterwards, cells were treated with vehicle (white bars) or BPA 1 nM (red bars) in the absence or presence of PHTPP 1 μM for 24 h. (**b**) Dispersed islet cells from WT and BERKO mice were treated with vehicle (white bars) or BPA (red bars) for 48 h. Apoptosis was evaluated using Hoechst 33,342 and propidium iodide staining. (**c-h**) INS-1E (**c-e**) and EndoC-βH1 cells (**f-h**) were transfected with siCTRL or with a siRNA targeting ERβ (si*Erβ* or si*ERβ*). Cells were treated with vehicle (white bars) or BPA 1 nM (red bars) for 24 h. (**c,f**) Protein expression was measured by western blot. Representative images of four independent experiments are shown. (**d,g**) Apoptosis was evaluated using Hoechst 33,342 and propidium iodide staining. (**e,h**) BPA-induced apoptosis data from Fig. 5d (**e**) and Fig. 5g (**h**) are presented as apoptotic index. Data are shown as means ± SEM of 3–5 independent experiments. (**a**) ** $p \leq 0.01$ and *** $p \leq 0.001$ vs untreated vehicle; ## $p \leq 0.01$ as indicated by bars. Two-way ANOVA. (**b**) *** $p \leq 0.001$ vs WT vehicle; ### $p \leq 0.001$ vs respective WT. Two-way ANOVA. (**d,g**) *** $p \leq 0.001$ vs siCTRL vehicle; # $p \leq 0.05$ and ### $p \leq 0.001$ as indicated by bars. Two-way ANOVA. (**e,h**) * $p \leq 0.05$ and *** $p \leq 0.001$ vs siCTRL, by two-tailed Student's *t* test.

homodimers and for the heterodimer (Supplementary Fig. 8), suggesting a high stability of the hormone within the LBD pocket in the homo and heterodimers. Conversely, BPA shows rapid structural rearrangements for both homodimers and heterodimers (Supplementary Fig. 8), a behavior previously shown for monomers (Li et al., 2018; Marroqui et al., 2021). This suggests a less stable binding of BPA compared to E2 for the three configurations of dimers.

To investigate the binding affinity of both ligands in homo and heterodimers, we analyzed the frequency distribution of the solvation binding energy values of E2 and BPA bound to each type of dimer (Wang et al., 2016) (Fig. 6g-i). Of note, positive values indicate strong ligand–protein binding (Marroqui et al., 2021). E2 binding to both homodimer cavities, LBD-ERαα (Fig. 6g) and LBD-ERββ (Fig. 6h), shows very similar values. In the heterodimer, however, the solvation energy values were higher for E2 binding to the ERα monomer forming the

heterodimer (75 kcal/mol) than for E2 binding to the ERβ monomer of the heterodimer (63 kcal/mol) (Fig. 6i). For BPA, the solvation binding energy values for homodimers were 30–35 kcal/mol for LBD-ERαα (Fig. 6g) and 55–60 kcal/mol for LBD-ERββ (Fig. 6i), which indicates that BPA showed higher affinity for ERββ than for ERαα. When we analyzed LBD-ERαβ, the frequency distribution of the solvation energy deviated from a Gaussian distribution, especially for BPA bound to the beta subunit of the heterodimer (Fig. 6i). This suggests a much lower BPA affinity for LBD-ERαβ compared with LBD-ERββ. In summary, these simulations indicate that BPA affinity is higher for ERββ than for ERαα and ERαβ. Binding of E2 should stabilize the three forms, preferentially ERαα, while BPA would mainly stabilize ERββ and, to a much lesser extent, ERαα and would not stabilize ERαβ.

To further explore how E2, BPA and G1 affect heterodimer formation, we performed an in situ proximity ligand assay (PLA) and

Fig. 5. A GPER crosstalk with ERα and ERβ induces apoptosis. (**a,b**) INS-1E (**a**) and EndoC-βH1 cells (**b**) were pre-treated with vehicle or antiestrogen ICI 182,780 1 μM for 3 h. Afterwards, cells were treated with vehicle (white bars) or G1 100 nM (blue bars) in the absence or presence of ICI 182,780 1 μM for 24 h. Apoptosis was evaluated using Hoechst 33,342 and propidium iodide staining. (**c,d**) INS-1E were transfected with siCTRL or with a siRNA targeting GPER (si*Gper1*). Cells were treated with vehicle (white bars) or G1 100 nM (blue bars) for 24 h. (**c**) Protein expression was measured by western blot. Representative images of four independent experiments are shown. (**d**) Apoptosis was evaluated using Hoechst 33,342 and propidium iodide staining. (**e-h**) INS-1E (**e,g**) and EndoC-βH1 cells (**f,h**) were pre-treated with vehicle, ERα antagonist MPP 100 nM (**e,f**) or ERβ antagonist PHTPP 1 μM (**g,h**) for 3 h. Afterwards, cells were treated with vehicle (white bars) or G1 100 nM (blue bars) in the absence or presence of MPP 100 nM (**e,f**) or PHTPP 1 μM (**g,h**) for 24 h. Apoptosis was evaluated using Hoechst 33,342 and propidium iodide staining. (**g,h**) INS-1E cells were transfected with siCTRL or siRNAs targeting ERα (si*Erα*) and ERβ (si*Erβ*) or ERα and ERβ simultaneously (si*Erα/Erβ*.) Cells were treated with vehicle (white bars) or G1 100 nM (blue bars) for 24 h. Apoptosis was evaluated using Hoechst 33,342 and propidium iodide staining. (**e**) Dispersed islet cells from WT and BERKO mice were treated with vehicle (white bars) or G1 100 nM (blue bars) for 48 h. Apoptosis was evaluated using Hoechst 33,342 and propidium iodide staining. Data are shown as means ± SEM of 4–5 independent experiments. (**a,b,e-h**) **$p \leq 0.01$ and ***$p \leq 0.001$ vs untreated vehicle; $^{\#\#\#}p \leq 0.001$ as indicated by bars. Two-way ANOVA. (**d,i**) *$p \leq 0.05$, **$p \leq 0.01$ and ***$p \leq 0.001$ vs siCTRL vehicle; $^{\#}p \leq 0.001$ as indicated by bars. Two-way ANOVA. (**j**) **$p \leq 0.01$ vs WT vehicle; $^{\#\#}p \leq 0.01$ as indicated by bars. Two-way ANOVA.
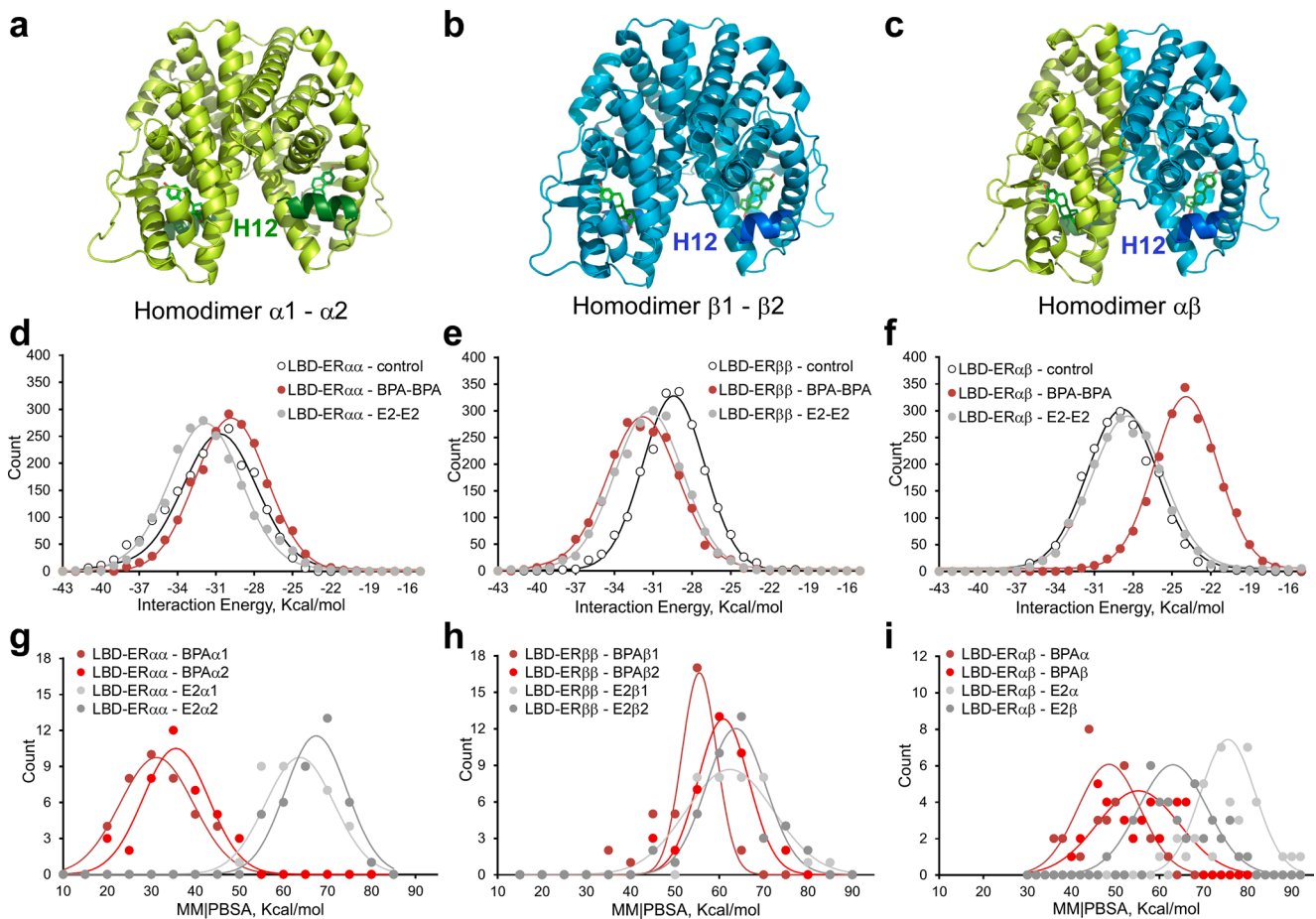
Fig. 6. Effect of BPA and E2 on the molecular dynamics for the LBD of the homodimer- or heterodimer-ER. Secondary structure models of closed LBD-ER as (**a**) alpha homodimer, (**b**) beta homodimer and (**c**) alpha–beta heterodimer. The H12 helix has been colored dark green (alpha monomers) or dark blue (beta monomers). The structure of E2 (green sticks for carbons) is included within the LBD cavities of both subunits. (**d**) Frequency distributions of the intermolecular protein Foldx-calculated interaction energy for the subunits of the alpha homodimer, (**e**) beta homodimer and (**f**) alfa-beta heterodimer in the presence of BPA or E2 ligands in each H12 closed LBD cavity. (**g**) Frequency distributions of the molecular mechanics Poisson–Boltzmann surface area (MM/PBSA) solvation binding energy values of each ligand bound to cavity of the alpha homodimer, (**h**) beta homodimer or (**i**) alpha–beta heterodimer in the presence of BPA or E2 ligands inside of the closed LBD. YASARA software-calculated MM|PBSA values more positive energies indicate better binding of the compound bound to the protein. A Gaussian curve overlaps discrete data.

coimmunoprecipitation. The PLA analysis showed a small number of heterodimers (shown as red dots) in vehicle-treated cells, which greatly increased upon E2 exposure for 24 h (Fig. 7a, Veh and E2 panels). In the presence of BPA or G1, however, very few red dots were observed, suggesting that these compounds decreased heterodimer formation (Fig. 7a, BPA and G1 panels). Coimmunoprecipitation assays indicated that ERα directly bound to ERβ (Fig. 7b-e). In agreement with the PLA data, the interaction between ERα and ERβ was augmented by E2 and significantly reduced by BPA (Fig. 7b, c) and G1 (Fig. 7d, e). Altogether, these results suggest that E2 promotes ERαβ heterodimerization, while BPA and G1 disrupt ERαβ formation.

4. Discussion

BPA is an endocrine disruptor with diabetogenic properties (Alonso-Magdalena et al., 2011; Sargis and Simmons, 2019). In adult mice, BPA increases serum insulin levels and induces insulin resistance (Alonso-Magdalena et al., 2006). In adult humans, BPA rapidly changed plasma insulin levels (Stahlhut et al., 2018), and epidemiological studies have linked BPA exposure to type 2 diabetes development (Rancière et al., 2019; Wang et al., 2019). When administered to pregnant mice, BPA altered insulin release, beta cell mass, and the metabolome in male offspring (Alonso-Magdalena et al., 2010; Bansal et al., 2017; Cabaton

et al., 2013) as well as altered glucose homeostasis in mothers later in life (Alonso-Magdalena et al., 2015, 2010). In vivo results demonstrating an increase in BPA-induced apoptosis are scarce. BPA exposure during pregnancy decreased beta cell mass and increased apoptosis six months after delivery (Alonso-Magdalena et al., 2015). Increased apoptosis and decreased beta cell mass were also described in first- and second-generation male offspring born to mothers treated with BPA during pregnancy (Bansal et al., 2017). In adult male mice treated with strep-tozotocin, BPA exacerbated endoplasmic reticulum stress in a mechanism involving altered Ca^{2+} signaling but did not induce apoptosis (Ahn et al., 2018). Here, we show that environmentally relevant doses of BPA increase beta cell apoptosis in an ERα-, ERβ-, and GPER-dependent manner. Furthermore, molecular dynamics simulations together with PLA and coimmunoprecipitation data indicate that BPA binding to ERα and ERβ, as well as GPER activation, decreased ERαβ heterodimers. Of note, the assessment of the in vivo effects of BPA on apoptosis in an animal model that may be linked to the findings described in this work is still missing and warrants further investigation.

It has been shown that E2 protects beta cells from several proapo-ptotic stimuli, such as oxidative stress (le May et al., 2006), proin-flammatory cytokines (Contreras et al., 2002) and high glucose (Kooptiwut et al., 2018). These studies suggest that ERα is crucial for pancreatic islet survival. For example, E2 prevented streptozotocin-
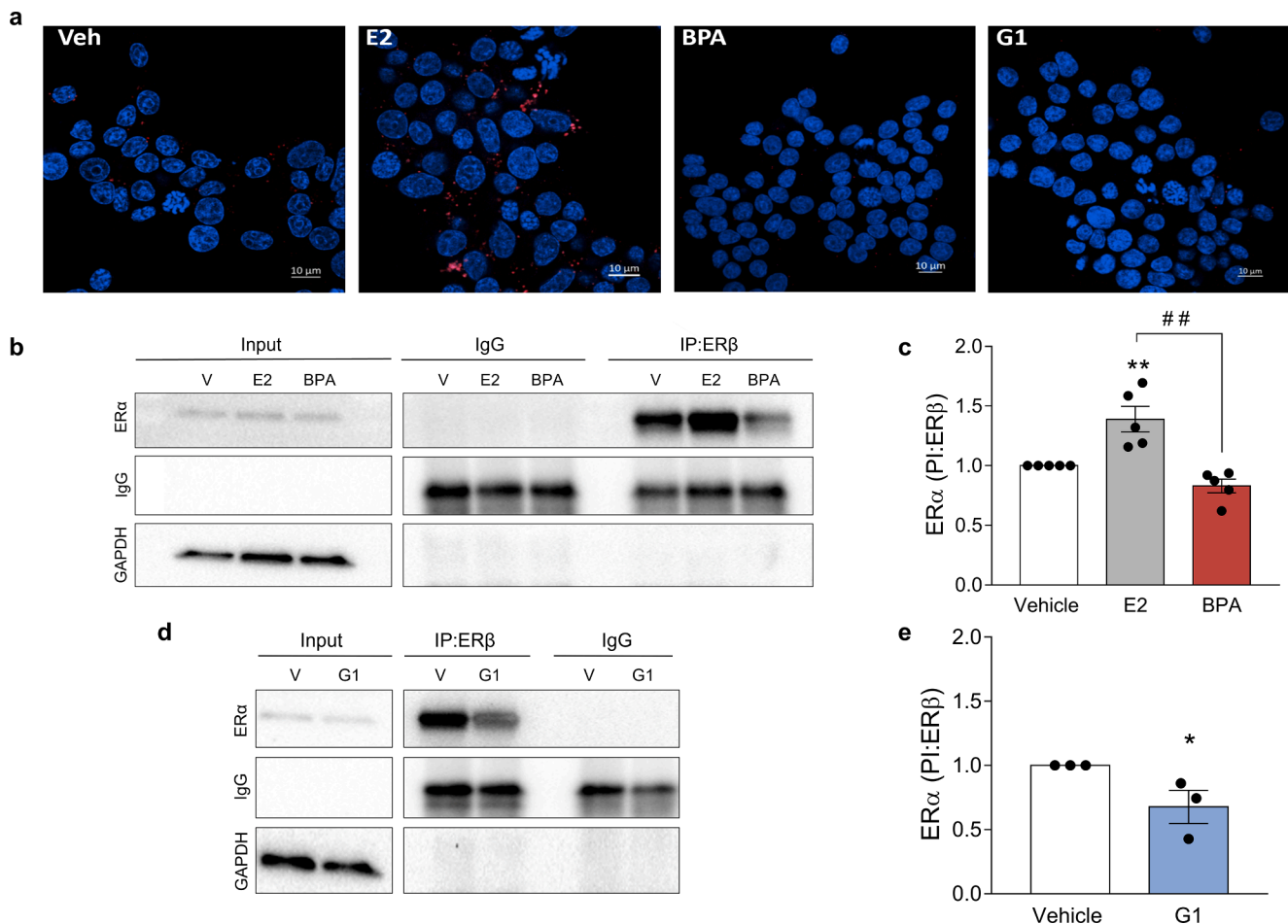
Fig. 7. E2 and BPA have differential effects on ERα/β heterodimer formation. (a) INS-1E cells were treated with vehicle, E2 1 nM, BPA 1 nM or G1 100 nM for 24 h. Heterodimers were detected using in situ proximity ligand assay, where heterodimers are represented as red dots (Texas red) and nuclei are shown in blue (DAPI). **(b-e)** INS-1 E cells were treated with vehicle (white bars), E2 1 nM (grey bars), BPA 1 nM (red bars) **(b,c)** or G1 100 nM (blue bars) **(d,e)** for 24 h. Cells were lysed and proteins collected for co-immunoprecipitation with anti-ERβ antibody. Nonspecific rabbit IgG was used as a negative control. Immunoprecipitates and total protein (Input) expression were measured by western blot. Representative images of three to five independent experiments are shown **(b,d)** and densitometry results are presented for ERα-specific binding to ERβ **(c,e)**. Values were normalised by GAPDH and then by the value of vehicle-treated cells of each experiment (considered as 1). Data are shown as means ± SEM of 3–5 independent experiments. **(c)** $**p \leq 0.01$ vs vehicle; $^{##}p \leq 0.01$ as indicated by bars. One-way ANOVA. **(e)** $*p \leq 0.05$ vs vehicle, by two-tailed Student's t test.

induced beta cell apoptosis in vivo and protected mice from insulin-deficient diabetes in an ERα-dependent manner (le May et al., 2006). Furthermore, ERα preserved mitochondrial function and attenuated endoplasmic reticulum stress in a context where ERα silencing promoted ROS production and induced beta cell apoptosis (Zhou et al., 2018). Here, ERα knockdown or treatment with the ERα antagonist MPP induced beta cell apoptosis, reinforcing an antiapoptotic role of this receptor even in the absence of added ligands. In the presence of ER ligands, we observed two different scenarios: while an ERα agonist had no effect on viability, BPA induced ROS production and beta cell apoptosis, indicating that BPA disrupts the ERα antiapoptotic role. Our findings indicate that ERβ also plays a pro-survival role in beta cells because either its silencing or antagonism with PHTPP leads to apoptosis. Interestingly, the percentage of apoptosis in ERβ-silenced cells was much higher than that in ERα-deficient cells, suggesting that ERβ may be more important for beta cell survival. The BPA effect on apoptosis was abrogated in ERβ-inhibited cells, indicating that ERβ is also involved in BPA-induced apoptosis. The antiapoptotic protection conferred by ERs is in line with previous findings in islets from ERα- and ERβ-knockout mice (Liu et al., 2009).

After ligand binding, ERα and ERβ form homo and heterodimers to exert their biological effects (Levin and Hammes, 2016). Different ER ligands stabilize ERα and ERβ homo and heterodimers in a variety of combinations that mediate the effect of those ER ligands (Paulmurugan et al., 2011). Our bioinformatic results predicted that E2 favors the formation of ERαα, ERββ and ERαβ. BPA, however, stabilized ERββ but did not stabilize ERαβ heterodimers. Based on these results, we proposed a model where ERαα, ERββ and ERαβ are antiapoptotic under basal conditions. Upon binding, E2 favors ERαβ heterodimers as well as ERαα and ERββ homodimers, thus protecting beta cells from apoptosis. Conversely, ERαβ heterodimer formation does not occur in the presence of BPA; in fact, the number of ERαβ heterodimers is even decreased by BPA exposure. How can the change in the degree of ERαβ hetero-dimerization influence apoptosis levels? With the experiments described in this work, we cannot know exactly, but we can speculate that the nonformation of heterodimers in the presence of BPA or G1 will increase the proportion of free ERα and ERβ that could form dimers of ERαα and ERββ in the presence of BPA and, according to our bioinformatics data, preferentially ERββ. This modification of the dimer and heterodimer populations may lead to a lower basal protection from apoptosis, visualized in our experiments as an increase in apoptosis (Fig. 8). Another possibility that we cannot rule out is that in the presence of E2 or BPA, different combinations of heterodimers are formed with the five existing isoforms of ERβ. In this work, we show the presence of ERβ isoforms in
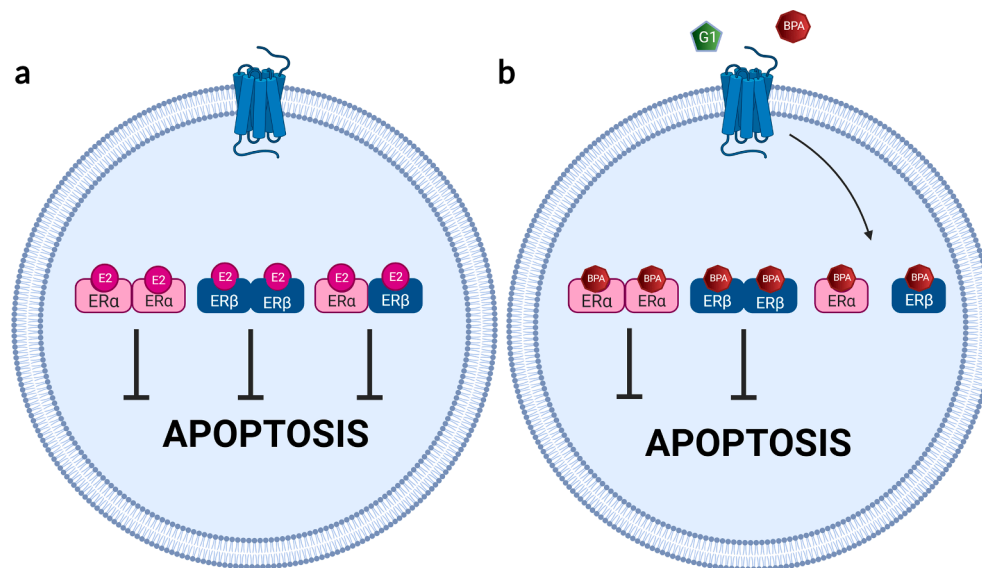
Fig. 8. Scheme summarizing our model for E2 and BPA effects on beta cell apoptosis. (**a**) In basal conditions, ERα, ERβ homodimers and ERαβ heterodimers exist and protect beta cells from apoptosis. These dimers are also stabilized by E2. (**b**) Activation of GPER by G1 or BPA decreases ERαβ heterodimers and increases apoptosis. Binding of BPA to ERα and/or ERβ disfavors ERαβ formation. Created with BioRender.com.

pancreatic beta cells (ESM 5). It has been previously shown that different ERβ isoforms can give rise to opposite effects even in the same cell type (Leung et al., 2006; Yan et al., 2021). This possibility warrants further study.

A direct effect of BPA on ERα and ERβ heterodimerization may explain the part of the BPA apoptotic effect that is neither blocked by GPER antagonism nor fully achieved by GPER activation. Nonetheless, we demonstrated that GPER activation by either BPA or G1 contributes to beta cell apoptosis. Because BPA binds to GPER in other cell systems (Thomas and Dong, 2006) and induces rapid nongenomic effects (Chevalier et al., 2014), it is plausible to assume that BPA acts as a GPER agonist in beta cells. Both cell lines expressed GPER mRNA and protein to a higher extent than ERα and ERβ. Quantification of protein levels between both cell lines is difficult with the present data; nonetheless, there is a trend to higher levels of GPER in EndoC-βH1 compared to INS-1E. This may explain why the effect of G1 was stronger in the human cell line than in the rat cell line. In any case, similar results were obtained throughout the whole manuscript despite the differences in GPER expression between both cell lines.

Because the G1 and BPA effects were abolished in the presence of an ER antagonist, after ER knockdown and in islet cells from BERKO mice, we suggest that ERα and ERβ are responsible for the effect of GPER activation. Remarkably, E2, which binds to and activates GPER (Revankar et al., 2005; Thomas et al., 2005), does not behave as G1 or BPA. The reason for these differences remains elusive. Crosstalk between GPER and ERα has been described for E2 and environmental estrogens (Qie et al., 2021). GPER interacts with ERα signaling directly by physical association and indirectly by GPER activity, modifying ERα expression and/or function (Romano and Gorelick, 2018). Crosstalk with ERβ has been less studied, and in this work, the mode of crosstalk is another open question for future studies.

Thus, along with BPA effects on insulin secretion and insulin sensitivity, the BPA-induced apoptosis described by us (present data) and others (Carchia et al., 2015; Lin et al., 2013) may contribute to elucidating the diabetogenic effects of BPA described above. In this work, BPA induces apoptosis at doses within the picomolar and nanomolar ranges, which agrees with both in vivo and in vitro studies showing that BPA has effects at low doses (Soto et al., 2021; vom Saal and Vandenberg, 2021). Although BPA shows a low affinity for ERα and ERβ (Kuiper et al., 1998; Molina-Molina et al., 2013) and binds to GPER with an IC$_{50}$ of 630 nM (Thomas and Dong, 2006), it is plausible to expect that an

amplification of the response to BPA caused by the crosstalk among the three ERs contributes to the proapoptotic effect induced by low concentrations of BPA.

Currently, there is a lack of methods for testing EDCs that disrupt metabolism and metabolic functions (Legler et al., 2020). The MIE triggered by BPA and the subsequent increase in ROS production should help to develop novel cellular testing methods to identify other EDCs with diabetogenic properties. Moreover, our results reinforce the need to incorporate ERα and ERβ homodimer and heterodimer formation in tests to identify EDCs, as has been already proposed for ERα dimer formation (Kim et al., 2021). Finally, the MIE described herein reflects the complexity of the molecular mechanisms underlying EDC actions. Such complexity complicates the prediction of a given EDC effect without having exact knowledge of the MIE involved. Acquiring this knowledge is a long-term goal; therefore, a deep understanding of MIEs should not be a strict requirement to create public health policies on EDCs (Soto and Sonnenschein, 2018).

5. Conclusions

The three estrogen receptors, ERα, ERβ and GPER, protect beta cells from apoptosis under basal conditions. Low doses of BPA increased beta cell apoptosis in three different cell models, i.e., dispersed mouse islet cells, the rat beta cell line INS-1E, and the human beta cell line EndoC-βH1. Our data indicate that EndoC-βH1 cells work as a proper human cell model for the identification of EDCs with diabetogenic activity.

The proapoptotic effect of BPA involves crosstalk among the three estrogen receptors. Activation of GPER by G1 or BPA induced apoptosis via ERα and ERβ. Our results indicate that BPA directly decreases ERαβ heterodimers via ERα and ERβ or after activation of GPER. This decrease in ERαβ heterodimers disrupts the active antiapoptotic effect of ERα and ERβ in beta cells. Our results should help to develop new test methods to identify diabetogenic EDCs based on the use of human EndoC-βH1 cells, GPER activation, ROS production, and homo and heterodimerization of ERα and ERβ.

Author contributions

LM and AN conceived the study. IB-C, RSDS, RMM-G, AAP-S, J-AE and LM collected and analyzed the data. IB-C, RSDS, RMM-G, AAP-S, J-AE, JM-P, LM and AN interpreted the data. RSDS, JM-P and AN drafted

the manuscript. AN and LM supervised the study. RSDS, JM-P, J-AG critically revised the manuscript for important intellectual content. J-AG, J-AE, LM, JM-P and AN acquired the funding. All authors reviewed and approved the final version of the manuscript and gave consent for publication. LM and AN are responsible for the integrity of the work as a whole.

Declaration of Competing Interest

Appendix A. Supplementary material

Supplementary data to this article can be found online at https://doi.org/10.1016/j.envint.2022.107250.

References

Ahn, C., Kang, H.-S., Lee, J.-H., Hong, E.-J., Jung, E.-M., Yoo, Y.-M., Jeung, E.-B., 2018. Bisphenol A and octylphenol exacerbate type 1 diabetes mellitus by disrupting calcium homeostasis in mouse pancreas. Toxicol. Lett. 295, 162–172.

Allen, T.E.H., Goodman, J.M., Gutsell, S., Russell, P.J., 2014. Defining Molecular Initiating Events in the Adverse Outcome Pathway Framework for Risk Assessment. Chem. Res. Toxicol. 27, 2100–2112. https://doi.org/10.1021/tx500345j.

Alonso-Magdalena, P., García-Arévalo, M., Quesada, I., Nadal, Á., 2015. Bisphenol-A treatment during pregnancy in mice: A new window of susceptibility for the development of diabetes in mothers later in life. Endocrinology (United States) 156 (5), 1659–1670.

Alonso-Magdalena, P., Morimoto, S., Ripoll, C., Fuentes, E., Nadal, A., 2006. The estrogenic effect of bisphenol A disrupts pancreatic beta-cell function in vivo and induces insulin resistance. Environ Health Perspect 114, 106–112. https://doi.org/10.1289/ehp.8451.

Alonso-Magdalena, P., Quesada, I., Nadal, A., 2011. Endocrine disruptors in the etiology of type 2 diabetes mellitus. Nat Rev Endocrinol 7, 346–353. https://doi.org/10.1038/nrendo.2011.56.

Alonso-Magdalena, P., Ropero, A.B., Carrera, M.P., Cederroth, C.R., Baquie, M., Gauthier, B.R., Nef, S., Stefani, E., Nadal, A., 2008. Pancreatic insulin content regulation by the estrogen receptor ER alpha. PLoS ONE 3, e2069. https://doi.org/10.1371/journal.pone.0002069.

Alonso-Magdalena, P., Vieira, E., Soriano, S., Menes, L., Burks, D., Quesada, I., Nadal, A., 2010. Bisphenol A exposure during pregnancy disrupts glucose homeostasis in mothers and adult male offspring. Environ Health Perspect 118, 1243–1250. https://doi.org/10.1289/ehp.1001993.

Balhuizen, A., Kumar, R., Amisten, S., Lundquist, I., Salehi, A., 2010. Activation of G protein-coupled receptor 30 modulates hormone secretion and counteracts cytokine-induced apoptosis in pancreatic islets of female mice. Mol. Cell. Endocrinol. 320, 16–24. https://doi.org/10.1016/j.mce.2010.01.030.

Bansal, A., Rashid, C., Xin, F., Li, C., Polyak, E., Duemler, A., van der Meer, T., Stefaniak, W., Wajid, S., Doliba, N., Bartolomei, M.S., Simmons, R.A., 2017. Sex- and dose-specific effects of maternal bisphenol A exposure on pancreatic islets of first- and second-generation adult mice offspring. Environ. Health Perspect. 125 (9), 097022.

Biasini, M., Bienert, S., Waterhouse, A., Arnold, K., Studer, G., Schmidt, T., Kiefer, F., Cassarino, T.G., Bertoni, M., Bordoli, L., Schwede, T., 2014. SWISS-MODEL: Modelling protein tertiary and quaternary structure using evolutionary information. Nucleic Acids Research 42. https://doi.org/10.1093/nar/gku340.

Cabaton, N.J., Canlet, C., Wadia, P.R., Tremblay-Franco, M., Gautier, R., Molina, J., Sonnenschein, C., Cravedi, J.-P., Rubin, B.S., Soto, A.M., Zalko, D., 2013. Effects of low doses of bisphenol A on the metabolome of perinatally exposed CD-1 mice. Environ Health Perspect 121, 586–593. https://doi.org/10.1289/ehp.1205588.

Carchia, E., Porreca, I., Almeida, P.J., D'Angelo, D., Cuomo, D., Ceccarelli, M., De Felice, M., Mallardo, M., Ambrosino, C., 2015. Evaluation of low doses BPA-induced perturbation of glycemia by toxicogenomics points to a primary role of pancreatic islets and to the mechanism of toxicity. Cell Death Dis. 6 (10), e1959.

Chevalier, N., Paul-Bellon, R., Camparo, P., Michiels, J.F., Chevallier, D., Fénichel, P., 2014. Genetic variants of GPER/GPR30, a novel estrogen-related G protein receptor, are associated with human seminoma. Int. J. Mol. Sci. 15, 1574–1589. https://doi.org/10.3390/ijms15011574.

Contreras, J.L., Smyth, C.A., Bilbao, G., Young, C.J., Thompson, J.A., Eckhoff, D.E., 2002. 17β-estradiol protects isolated human pancreatic islets against proinflammatory cytokine-induced cell death: Molecular mechanisms and islet functionality. Transplantation 74. https://doi.org/10.1097/00007890-200211150-00010.

Cunha, D.A., Cito, M., Carlsson, P.-O., Vanderwinden, J.-M., Molkentin, J.D., Bugliani, M., Marchetti, P., Eizirik, D.L., Cnop, M., 2016. Thrombospondin 1 protects pancreatic β-cells from lipotoxicity via the PERK-NRF2 pathway. Cell Death Differ. 23 (12), 1995–2006.

Delgado, J., Radusky, L.G., Cianferoni, D., Serrano, L., 2019. FoldX 5.0: Working with RNA, small molecules and a new graphical interface. Bioinformatics 35. https://doi.org/10.1093/bioinformatics/btz184.

Denizot, F., Lang, R., 1986. Rapid colorimetric assay for cell growth and survival. Modifications to the tetrazolium dye procedure giving improved sensitivity and reliability. J Immunol Methods 89, 271–277. https://doi.org/10.1016/0022-1759(86)90368-6.

Eizirik, D.L., Pasquali, L., Cnop, M., 2020. Pancreatic beta-cells in type 1 and type 2 diabetes mellitus: different pathways to failure. Nat Rev Endocrinol 16, 349–362. https://doi.org/10.1038/s41574-020-0355-7.

Gannon, M., Kulkarni, R.N., Tse, H.M., Mauvais-Jarvis, F., 2018. Sex differences underlying pancreatic islet biology and its dysfunction. Mol Metab 15, 82–91. https://doi.org/10.1016/j.molmet.2018.05.017.

Gore, A.C., Chappell, V.A., Fenton, S.E., Flaws, J.A., Nadal, A., Prins, G.S., Toppari, J., Zoeller, R.T., 2015. EDC-2: The Endocrine Society's Second Scientific Statement on Endocrine-Disrupting Chemicals. Endocr. Rev. 36 (6), E1–E150.

Heldring, N., Pike, A., Andersson, S., Matthews, J., Cheng, G., Hartman, J., Tujague, M., Strom, A., Treuter, E., Warner, M., Gustafsson, J.A., 2007. Estrogen receptors: how do they signal and what are their targets. Physiol Rev 87, 905–931. https://doi.org/10.1152/physrev.00026.2006.

Iwabuchi, E., Miki, Y., Ono, K., Onodera, Y., Suzuki, T., Hirakawa, H., Ishida, T., Ohuchi, N., Sasano, H., 2017. In situ detection of estrogen receptor dimers in breast carcinoma cells in archival materials using proximity ligation assay (PLA). J Steroid Biochem Mol Biol 165, 159–169. https://doi.org/10.1016/j.jsbmb.2016.05.022.

Kang, L., Zhang, X., Xie, Y., Tu, Y., Wang, D., Liu, Z., Wang, Z.Y., 2010. Involvement of estrogen receptor variant ER-alpha36, not GPR30, in nongenomic estrogen signaling. Mol Endocrinol 24, 709–721. https://doi.org/10.1210/me.2009-0317.

Kautzky-Willer, A., Harreiter, J., Pacini, G., 2016. Sex and Gender Differences in Risk, Pathophysiology and Complications of Type 2 Diabetes Mellitus. Endocr Rev 37, 278–316. https://doi.org/10.1210/er.2015-1137.

Kim, H.M., Seo, H., Park, Y., Lee, H.-S., Lee, S.-H., Ko, K.S., 2021. Development of a Human Estrogen Receptor Dimerization Assay for the Estrogenic Endocrine-Disrupting Chemicals Using Bioluminescence Resonance Energy Transfer. Int J Environ Res Public Health 18 (16), 8875.

Kooptiwut, S., Kaewin, S., Semprasert, N., Sujjitjoon, J., Junking, M., Suksri, K., Yenchitsomanus, P. thai, 2018. Estradiol Prevents High Glucose-Induced β-cell Apoptosis by Decreased BTG2 Expression. Scientific Reports 8. https://doi.org/10.1038/s41598-018-30698-x.

Krege, J.H., Hodgin, J.B., Couse, J.F., Enmark, E., Warner, M., Mahler, J.F., Sar, M., Korach, K.S., Gustafsson, J.-Å., Smithies, O., 1998. Generation and reproductive phenotypes of mice lacking estrogen receptor β. Proc Natl Acad Sci U S A 95 (26), 15677–15682.

Kuiper, G.G., Carlsson, B., Grandien, K., Enmark, E., Haggblad, J., Nilsson, S., Gustafsson, J.A., 1997. Comparison of the ligand binding specificity and transcript tissue distribution of estrogen receptors alpha and beta. Endocrinology 138, 863–870. https://doi.org/10.1210/endo.138.3.4979.

Kuiper, G.G., Lemmen, J.G., Carlsson, B., Corton, J.C., Safe, S.H., van der Saag, P.T., van der Burg, B., Gustafsson, J.A., 1998. Interaction of estrogenic chemicals and phytoestrogens with estrogen receptor beta. Endocrinology 139, 4252–4263. https://doi.org/10.1210/endo.139.10.6216.

Legler, J., Zalko, D., Jourdan, F., Jacobs, M., Fromenty, B., Balaguer, P., Bourguet, W., Munic Kos, V., Nadal, A., Beausoleil, C., Cristobal, S., Remy, S., Ermler, S., Margiotta-Casaluci, L., Griffin, J.L., Blumberg, B., Chesné, C., Hoffmann, S., Andersson, P.L., Kamstra, J.H., 2020. The goliath project: Towards an internationally harmonised approach for testing metabolism disrupting compounds. Int. J. Mol. Sci. 21 (10), 3480.

le May, C., Chu, K., Hu, M., Ortega, C.S., Simpson, E.R., Korach, K.S., Tsai, M.J., Mauvais-Jarvis, F., 2006. Estrogens protect pancreatic beta-cells from apoptosis and prevent insulin-deficient diabetes mellitus in mice. Proc Natl Acad Sci U S A 103, 9232–9237. https://doi.org/10.1073/pnas.0602956103.

Leung, Y.-K., Mak, P., Hassan, S., Ho, S.-M., 2006. Estrogen receptor (ER)-β isoforms: A key to understanding ER-β signaling. Proc Natl Acad Sci U S A 103 (35), 13162–13167.

Levin, E.R., Hammes, S.R., 2016. Nuclear receptors outside the nucleus: extranuclear signalling by steroid receptors. Nat Rev Mol Cell Biol 17, 783–797. https://doi.org/10.1038/nrm.2016.122.

Lin, Y., Sun, X., Qiu, L., Wei, J., Huang, Q., Fang, C., Ye, T., Kang, M., Shen, H., Dong, S., 2013. Exposure to bisphenol A induces dysfunction of insulin secretion and apoptosis through the damage of mitochondria in rat insulinoma (INS-1) cells. Cell Death Dis 4, e460. https://doi.org/10.1038/cddis.2012.206.

Liu, S., le May, C., Wong, W.P., Ward, R.D., Clegg, D.J., Marcelli, M., Korach, K.S., Mauvais-Jarvis, F., 2009. Importance of extranuclear estrogen receptor-alpha and membrane G protein-coupled estrogen receptor in pancreatic islet survival. Diabetes 58, 2292–2302. https://doi.org/10.2337/db09-0257.

Li, Y., Perera, L., Coons, L.A., Burns, K.A., Tyler Ramsey, J., Pelch, K.E., Houtman, R., van Beuningen, R., Teng, C.T., Korach, K.S., 2018. Differential in vitro biological action, coregulator interactions, and molecular dynamic analysis of bisphenol A (BPA), BPAF, and BPS ligand–ERα complexes. Environ. Health Perspect. 126 (1), 017012.

Marroqui, L., Dos Santos, R.S., Fløyel, T., Grieco, F.A., Santin, I., Op de beeck, A., Marselli, L., Marchetti, P., Pociot, F., Eizirik, D.L., 2015. TYK2, a Candidate Gene for Type 1 Diabetes, Modulates Apoptosis and the Innate Immune Response in Human Pancreatic β-Cells. Diabetes 64 (11), 3808–3817.

Marroqui, L., Martinez-Pinna, J., Castellano-Munoz, M., dos Santos, R.S., Medina-Gali, R. M., Soriano, S., Quesada, I., Gustafsson, J.A., Encinar, J.A., Nadal, A., 2021. Bisphenol-S and Bisphenol-F alter mouse pancreatic beta-cell ion channel expression and activity and insulin release through an estrogen receptor ERbeta mediated pathway. Chemosphere 265, 129051. https://doi.org/10.1016/j.chemosphere.2020.129051.

Martinez-Pinna, J., Marroqui, L., Hmadcha, A., Lopez-Beas, J., Soriano, S., Villar-Pazos, S., Alonso-Magdalena, P., dos Santos, R.S., Quesada, I., Martin, F., Soria, B., Gustafsson, J.A., Nadal, A., 2019. Oestrogen receptor beta mediates the actions of bisphenol-A on ion channel expression in mouse pancreatic beta cells. Diabetologia 62, 1667–1680. https://doi.org/10.1007/s00125-019-4925-y.

Molina-Molina, J.-M., Amaya, E., Grimaldi, M., Sáenz, J.-M., Real, M., Fernández, M.F., Balaguer, P., Olea, N., 2013. In vitro study on the agonistic and antagonistic activities of bisphenol-S and other bisphenol-A congeners and derivatives via nuclear receptors. Toxicol. Appl. Pharmacol. 272 (1), 127–136.

Mosmann, T., 1983. Rapid colorimetric assay for cellular growth and survival: application to proliferation and cytotoxicity assays. J Immunol Methods 65, 55–63. https://doi.org/10.1016/0022-1759(83)90303-4.

Paulmurugan, R., Tamrazi, A., Massoud, T.F., Katzenellenbogen, J.A., Gambhir, S.S., 2011. In vitro and in vivo molecular imaging of estrogen receptor α and β homo-and heterodimerization: Exploration of new modes of receptor regulation. Mol. Endocrinol. 25, 2029–2040. https://doi.org/10.1210/me.2011-1145.

Qie, Y.u., Qin, W., Zhao, K., Liu, C., Zhao, L., Guo, L.-H., 2021. Environmental Estrogens and Their Biological Effects through GPER Mediated Signal Pathways. Environ. Pollut. 278, 116826.

Rancière, Fanny, Botton, J., Slama, R., Lacroix, M.Z., Debrauwer, L., Charles, M.A., Roussel, Ronan, Balkau, Beverley, Magliano, D.J., Balkau, B., Ducimetière, P., Eschwège, E., Rancière, F., Alhenc-Gelas, F., Girault, A., Fumeron, F., Marre, M., Roussel, R., Bonnet, F., Bonnefond, A., Cauchi, S., Froguel, P., Alençon, Angers, Blois, Caen, Chateauroux, Chartres, Cholet, le Mans, Orléans, Tours, Cogneau, J., Born, C., Caces, E., Cailleau, M., Lantieri, O., Moreau, J.G., Rakotozafy, F., Tichet, J., Vol, S., 2019. Exposure to bisphenol a and bisphenol s and incident type 2 diabetes: A case-cohort study in the French cohort D.E.S.I.R. Environmental Health Perspectives 127. https://doi.org/10.1289/EHP5159.

Ravassard, P., Hazhouz, Y., Pechberty, S., Bricout-Neveu, E., Armanet, M., Czernichow, P., Scharfmann, R., 2011. A genetically engineered human pancreatic β cell line exhibiting glucose-inducible insulin secretion. Journal of Clinical Investigation 121 (9), 3589–3597.

Razandi, M., Pedram, A., Merchenthaler, I., Greene, G.L., Levin, E.R., 2004. Plasma membrane estrogen receptors exist and functions as dimers. Mol Endocrinol 18, 2854–2865. https://doi.org/10.1210/me.2004-0115.

Revankar, C.M., Cimino, D.F., Sklar, L.A., Arterburn, J.B., Prossnitz, E.R., 2005. A transmembrane intracellular estrogen receptor mediates rapid cell signaling. Science 1979 (307), 1625–1630. https://doi.org/10.1126/science.1106943.

Romano, S.N., Gorelick, D.A., 2018. Crosstalk between nuclear and G protein-coupled estrogen receptors. Gen. Comp. Endocrinol. 261, 190–197. https://doi.org/10.1016/j.ygcen.2017.04.013.

Santin, I., dos Santos, R.S., Eizirik, D.L., 2016. Pancreatic beta cell survival and signaling pathways: Effects of type 1 diabetes-associated genetic variants, in: Methods in Molecular Biology. https://doi.org/10.1007/7651_2015_291.

Sargis, R.M., Simmons, R.A., 2019. Environmental neglect: endocrine disruptors as underappreciated but potentially modifiable diabetes risk factors. Diabetologia 62, 1811–1822. https://doi.org/10.1007/s00125-019-4940-z.

Schmittgen, T.D., Livak, K.J., 2008. Analyzing real-time PCR data by the comparative C (T) method. Nat Protoc 3, 1101–1108. https://doi.org/10.1038/nprot.2008.73.

Soriano, S., Alonso-Magdalena, P., Garcia-Arevalo, M., Novials, A., Muhammed, S.J., Salehi, A., Gustafsson, J.A., Quesada, I., Nadal, A., 2012. Rapid insulinotropic action of low doses of bisphenol-A on mouse and human islets of Langerhans: role of estrogen receptor beta. PLoS ONE 7, e31109. https://doi.org/10.1371/journal.pone.0031109.

Soto, A.M., Schaeberle, C.M., Sonnenschein, C., 2021. From Wingspread to CLARITY: a personal trajectory. Nat Rev Endocrinol 17, 247–256. https://doi.org/10.1038/s41574-020-00460-3.

Soto, A.M., Sonnenschein, C., 2018. Endocrine disruptors - putting the mechanistic cart before the phenomenological horse. Nat Rev Endocrinol 14, 317–318. https://doi.org/10.1038/s41574-018-0003-7.

Stahlhut, R.W., Myers, J.P., Taylor, J.A., Nadal, A., Dyer, J.A., vom Saal, F.S., 2018. Experimental BPA exposure and glucose-stimulated insulin response in adult men and women. J Endocr Soc 2. https://doi.org/10.1210/js.2018-00151.

Thomas, P., Dong, J., 2006. Binding and activation of the seven-transmembrane estrogen receptor GPR30 by environmental estrogens: A potential novel mechanism of endocrine disruption. J. Steroid Biochem. Mol. Biol. 102, 175–179. https://doi.org/10.1016/j.jsbmb.2006.09.017.

Thomas, P., Pang, Y., Filardo, E.J., Dong, J., 2005. Identity of an estrogen membrane receptor coupled to a G protein in human breast cancer cells. Endocrinology 146, 624–632. https://doi.org/10.1210/en.2004-1064.

Tovchigrechko, A., Vakser, I.A., 2006. GRAMM-X public web server for protein-protein docking. Nucleic Acids Res. 34 (Web Server), W310–W314.

Tsonkova, V.G., Sand, F.W., Wolf, X.A., Grunnet, L.G., Kirstine Ringgaard, A., Ingvorsen, C., Winkel, L., Kalisz, M., Dalgaard, K., Bruun, C., Fels, J.J., Helgstrand, C., Hastrup, S., Öberg, F.K., Vernet, E., Sandrini, M.P.B., Shaw, A.C., Jessen, C., Grønborg, M., Hald, J., Willenbrock, H., Madsen, D., Wernersson, R., Hansson, L., Jensen, J.N., Plesner, A., Alanentalo, T., Petersen, M.B.K., Grapin-Botton, A., Honoré, C., Ahnfelt-Rønne, J., Hecksher-Sørensen, J., Ravassard, P., Madsen, O.D., Rescan, C., Frogne, T., 2018. The EndoC-βH1 cell line is a valid model of human beta cells and applicable for screenings to identify novel drug target candidates. Mol Metab 8, 144–157. https://doi.org/10.1016/j.molmet.2017.12.007.

Vandenberg, L.N., Chahoud, I., Heindel, J.J., Padmanabhan, V., Paumgartten, F.J., Schoenfelder, G., 2010. Urinary, circulating, and tissue biomonitoring studies indicate widespread exposure to bisphenol A. Environ Health Perspect 118, 1055–1070. https://doi.org/10.1289/ehp.0901716.

Villar-Pazos, S., Martinez-Pinna, J., Castellano-Muñoz, M., Alonso-Magdalena, P., Marroqui, L., Quesada, I., Gustafsson, J.-A., Nadal, A., 2017. Molecular mechanisms involved in the non-monotonic effect of bisphenol-a on ca2+ entry in mouse pancreatic β-cells. Sci. Rep. 7 https://doi.org/10.1038/s41598-017-11995-3.

vom Saal, F.S., Vandenberg, L.N., 2021. Update on the Health Effects of Bisphenol A: Overwhelming Evidence of Harm. Endocrinology 162. https://doi.org/10.1210/endocr/bqaa171.

Wang, B., Li, M., Zhao, Z., Lu, J., Chen, Y., Xu, Y., Xu, M., Wang, W., Wang, T., Bi, Y., Ning, G., 2019. Urinary bisphenol A concentration and glucose homeostasis in non-diabetic adults: a repeated-measures, longitudinal study. Diabetologia 62, 1591–1600. https://doi.org/10.1007/s00125-019-4898-x.

Wang, C., Nguyen, P.H., Pham, K., Huynh, D., Le, T.B., Wang, H., Ren, P., Luo, R., 2016. Calculating protein-ligand binding affinities with MMPBSA: Method and error analysis. J Comput Chem 37, 2436–2446. https://doi.org/10.1002/jcc.24467.

Yan, S., Dey, P., Ziegler, Y., Jiao, X., Kim, S.H., Katzenellenbogen, J.A., Katzenellenbogen, B.S., 2021. Contrasting activities of estrogen receptor beta isoforms in triple negative breast cancer. Breast Cancer Res. Treat. 185 (2), 281–292.

Zhou, Z., Ribas, V., Rajbhandari, P., Drew, B.G., Moore, T.M., Fluitt, A.H., Reddish, B.R., Whitney, K.A., Georgia, S., Vergnes, L., Reue, K., Liesa, M., Shirihai, O., van der Bliek, A.M., Chi, N.W., Mahata, S.K., Tiano, J.P., Hewitt, S.C., Tontonoz, P., Korach, K.S., Mauvais-Jarvis, F., Hevener, A.L., 2018. Estrogen receptor protects pancreatic -cells from apoptosis by preserving mitochondrial function and suppressing endoplasmic reticulum stress. J. Biol. Chem. 293, 4735–4751. https://doi.org/10.1074/jbc.M117.805069.